ACS OMEGA

Article

Cite This: ACS Omega 2018, 3, 6673−6682

Synthesis of Unsaturated Precursors for Parahydrogen-Induced Polarization and Molecular Imaging of 1-^{13}C-Acetates and 1-^{13}C-Pyruvates via Side Arm Hydrogenation

Nikita V. Chukanov,[†,‡] Oleg G. Salnikov,[†,‡] Roman V. Shchepin,[§] Kirill V. Kovtunov,[†,‡] Igor V. Koptyug,[†,‡] and Eduard Y. Chekmenev*[,§,∥,⊥]

[†]International Tomography Center, SB RAS, Institutskaya Street 3A, Novosibirsk 630090, Russia

[‡]Novosibirsk State University, Pirogova Street 2, Novosibirsk 630090, Russia

[§]Vanderbilt University Institute of Imaging Science (VUIIS), Department of Radiology, Department of Biomedical Engineering, and Vanderbilt-Ingram Cancer Center (VICC), Vanderbilt University, Nashville, Tennessee 37232-2310, United States

[∥]Russian Academy of Sciences, Leninskiy Prospekt 14, Moscow 119991, Russia

[⊥]Department of Chemistry, Integrative Biosciences (Ibio), Wayne State University, Karmanos Cancer Institute (KCI), Detroit, Michigan 48202, United States

Supporting Information

ABSTRACT: Hyperpolarized forms of 1-^{13}C-acetates and 1-^{13}C-pyruvates are used as diagnostic contrast agents for molecular imaging of many diseases and disorders. Here, we report the synthetic preparation of 1-^{13}C isotopically enriched and pure from solvent acetates and pyruvates derivatized with unsaturated ester moiety. The reported unsaturated precursors can be employed for NMR hyperpolarization of 1-^{13}C-acetates and 1-^{13}C-pyruvates via parahydrogen-induced polarization (PHIP). In this PHIP variant, Side arm hydrogenation (SAH) of unsaturated ester moiety is followed by the polarization transfer from nascent parahydrogen protons to ^{13}C nucleus via magnetic field cycling procedure to achieve hyperpolarization of ^{13}C nuclear spins. This work reports the synthesis of PHIP-SAH precursors: vinyl 1-^{13}C-acetate (55% yield), allyl 1-^{13}C-acetate (70% yield), propargyl 1-^{13}C-acetate (45% yield), allyl 1-^{13}C-pyruvate (60% yield), and propargyl 1-^{13}C-pyruvate (35% yield). Feasibility of PHIP-SAH ^{13}C hyperpolarization was verified by ^{13}C NMR spectroscopy: hyperpolarized allyl 1-^{13}C-pyruvate was produced from propargyl 1-^{13}C-pyruvate with ^{13}C polarization of ∼3.2% in CD_3OD and ∼0.7% in D_2O. ^{13}C magnetic resonance imaging is demonstrated with hyperpolarized 1-^{13}C-pyruvate in aqueous medium.

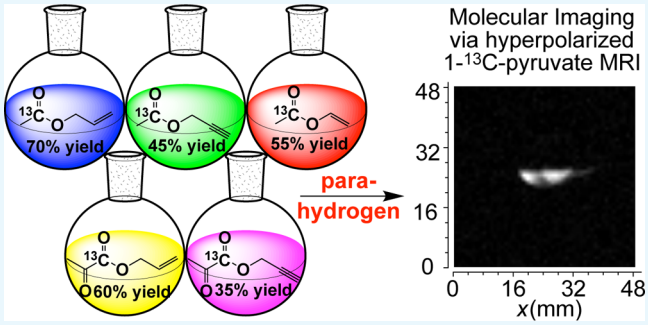

INTRODUCTION

NMR hyperpolarization techniques enhance nuclear spin polarization by orders of magnitude with corresponding gains in NMR and magnetic resonance imaging (MRI) detection sensitivities.[1−6] The produced hyperpolarized (HP) biomolecules can be employed as molecular contrast agents to probe in vivo metabolism and function.[6−12]

^{13}C hyperpolarized 1-^{13}C-pyruvate and its derivatives are of particular importance because the injection of HP pyruvate-1-^{13}C and molecular imaging of its metabolic product HP 1-^{13}C-lactate can report on tumor metabolism,[8] tumor grading[13] and response to treatment,[14,15] and other applications.[16−18] HP 1-^{13}C-pyruvate is now in clinical trials.[19]

Another similar compound is HP 1-^{13}C-acetate, which can be useful for probing brain and liver metabolism.[20−23] For example, Mishkovsky and co-workers performed in vivo detection of brain Krebs cycle intermediate by hyperpolarized magnetic resonance using HP 1-^{13}C-acetate.[24] Moreover, Jensen and co-workers performed a study on tissue-specific short-chain fatty acid metabolism and slow metabolic recovery in liver using injection of HP 1-^{13}C-acetate.[25]

Hyperpolarization of carboxyl ^{13}C nuclei (compared to proton hyperpolarization) in these molecular frameworks is advantageous due to significantly longer hyperpolarization lifetime in vivo (by approximately an order of magnitude) and negligible ^{13}C in vivo background signal. Moreover, carboxyl ^{13}C (unlike other carbons in these frameworks) has the largest dispersion of the isotropic chemical shift, making it a sensitive probe of the structural and environmental changes.[2,6,8]

These two HP contrast agents were first hyperpolarized using dissolution dynamic nuclear polarization (d-DNP) technique,[12,26] which relies on polarization transfer from

Received: May 12, 2018
Accepted: June 8, 2018
Published: June 20, 2018

DOI: 10.1021/acsomega.8b00983
ACS Omega 2018, 3, 6673−6682

unpaired electrons at cryogenic temperatures and high magnetic fields.[27]

Parahydrogen-induced polarization (PHIP) is an alternative hyperpolarization technique.[28−31] In PHIP, parahydrogen (pH_2) is added in a pairwise manner (two hydrogen atoms from the same parahydrogen molecule end up in the same product molecule) to unsaturated precursor compound.[28−31] Next, polarization is transferred from nascent parahydrogen protons to ^{13}C nucleus via spin−spin couplings.[10,11,32−36] A number of ^{13}C PHIP-HP contrast agents have been developed[37−39] and validated in vivo over the years.[40−52] However, ^{13}C hyperpolarization of pyruvate and acetate remained challenging due to restricting chemistry of PHIP precursor molecules until the side arm hydrogenation (SAH) technique was pioneered by Reineri, Aime, and co-workers.[53−55] In PHIP-SAH (Scheme 1), pH_2 is added in a pairwise manner to ester moiety.[53−59] Next, polarization transfer from nascent parahydrogen protons is accomplished via magnetic field cycling (MFC) procedure.[36] During MFC, the magnetic field is decreased to nanotesla range first and adiabatically swept to the field above a few microtesla (typically to the Earth's magnetic field of ca. 50 μT because of the practical convenience).[10,11,34] As a result, the spin−spin couplings between nascent parahydrogen protons and ^{13}C carboxyl nucleus enable efficient hyperpolarization of ^{13}C carboxyl site.[10,11,34] Polarization up to 20−50% is theoretically feasible for acetate and pyruvate molecular frameworks.[53,56]

Scheme 1. Schematic Diagram of ^{13}C Hyperpolarization via Parahydrogen-Induced Polarization (PHIP) via Side Arm Hydrogenation (SAH)[a]

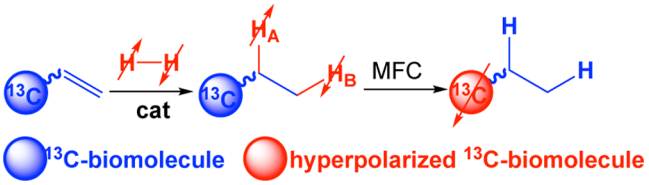

[a]Parahydrogen is added in a pairwise manner in the first step to the unsaturated ester moiety. In the second step, the reaction product undergoes the magnetic field cycling (MFC) procedure when static magnetic field is rapidly reduced to a nanotesla range first and then the static magnetic field is adiabatically ramped to a microtesla range (typically the Earth's magnetic field of ca. 50 μT for practical convenience).

Preparation of pure HP ^{13}C aqueous solutions of de-esterified pyruvates and acetates has been demonstrated in the context of PHIP-SAH (with residual ^{13}C polarization between 3 and 5%,[55] which can be additionally improved in the future through the use of automated high-pressure hyperpolarizers in principle[36,50,60,61]) for future in vivo and clinical use.

In this work, we provide a systematic synthetic report for the preparation of ^{13}C molecular precursors for PHIP-SAH of pyruvate and acetate with allyl, propargyl, and vinyl moieties (Scheme 2). These moieties have been shown to be efficient for pairwise hydrogenation reactions and polarization transfer from nascent parahydrogen-derived protons to ^{13}C carboxyl nuclei.[55] We anticipate the reported synthetic protocols to be of practical experimental use for those trying to establish HP imaging programs for in vivo molecular imaging of cancer, brain and liver metabolism, and other biomedical studies.

Scheme 2. Chemical Structures of Key Reagents and All Molecular Precursors Prepared in This Study for PHIP-SAH Hyperpolarization of ^{13}C Carboxyl Sites[a]

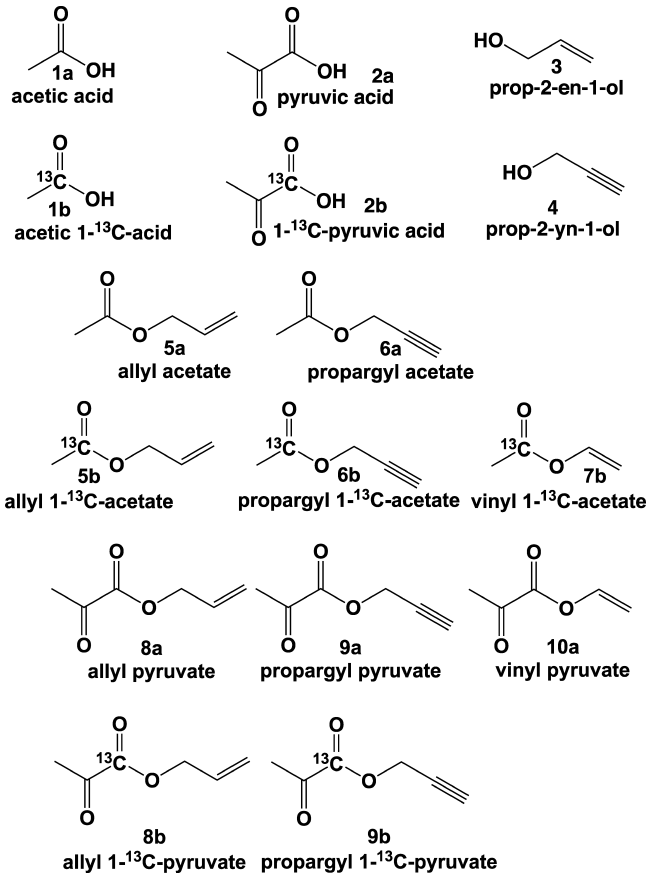

[a]Note ^{13}C label depicts ~98% ^{13}C enrichment, while no label assumes natural ^{13}C abundance of ~1.1%.

EXPERIMENTAL DETAILS

General Procedure A for the Synthesis of Allyl and Propargyl Acetates. Acetic acid (0.25−0.30 mol, 1 equiv), alcohol (1.1 equiv), and *p*-TsOH (0.05−0.10 equiv) were mixed in a 50 mL round-bottom flask equipped with a Dean−Stark adapter and condenser. The apparatus was flushed with argon, and the reaction mixture was refluxed for 4−8 h until 1 equiv of water was collected in the trap of the Dean−Stark adapter. After cooling, the reaction mixture was washed with 2 × 50 mL of saturated $NaHCO_3$ solution and 2 × 50 mL of saturated NaCl solution and dried with anhydrous $CaCl_2$. The product was distilled at atmospheric pressure.

Allyl Acetate 5a. Allyl acetate **5a** was obtained using general procedure A from 15.3 g of acetic acid **1a**. The yield was 19 g (75%).

^1H NMR (400 MHz, $CDCl_3$): 5.84−5.91 (m, 1H), 5.27 (doublet of multiplets (dm), 1H, J = 17.2 Hz), 5.19 (dm, 1H, J = 10.5 Hz), 4.53 (dm, 2H, J = 5.9 Hz), 2.04 (s, 3H). ^{13}C NMR (100 MHz, $CDCl_3$): 170.8, 132.3, 118.3, 65.2, 21.0.

Propargyl Acetate 6a. Propargyl acetate **6a** was obtained using general procedure A from 20.0 g of acetic acid **1a**. The yield was 15 g (45%).

^1H NMR (400 MHz, $CDCl_3$): 4.62 (d, 2H, J = 2.5 Hz), 2.44 (t, 1H, J = 2.5 Hz), 2.06 (s, 3H). ^{13}C NMR (100 MHz, $CDCl_3$): 170.2, 77.7, 74.9, 52.0, 20.7.

DOI: 10.1021/acsomega.8b00983
ACS Omega 2018, 3, 6673−6682

Allyl 1-^{13}C-Acetate 5b. Allyl 1-^{13}C-acetate **5b** was synthesized using general procedure A from 15.0 g of 1-^{13}C-acetic acid **1b**. The yield was 17 g (70%).

^{1}H NMR (400 MHz, $CDCl_3$): 5.85−5.91 (m, 1H), 5.27 (dm, 1H, J = 17.2 Hz), 5.20 (dm, 1H, J = 10.5 Hz), 4.52−4.54 (m, 2H), 2.04 (d, 3H, J = 7.0 Hz). ^{13}C NMR (100 MHz, $CDCl_3$): 170.8, 132.3 (d, J = 2.5 Hz), 118.3, 65.2 (d, J = 2.5 Hz), 21.0 (d, J = 59.5 Hz).

Propargyl 1-^{13}C-Acetate 6b. Propargyl 1-^{13}C-acetate **6b** was obtained using general procedure A from 18.0 g of 1-^{13}C-acetic acid **1b**. The yield was 13 g (45%).

^{1}H NMR (400 MHz, $CDCl_3$): 4.63 (dd, 2H, J = 3.5 and 2.5 Hz), 2.44 (t, 1H, J = 2.5 Hz), 2.06 (d, 3H, J = 7.0 Hz). ^{13}C NMR (100 MHz, $CDCl_3$): 170.2, 77.7 (d, J = 2.8 Hz), 74.9, 52.0 (d, J = 2.6 Hz), 20.7 (d, J = 59.4 Hz).

Preparation Procedure for Vinyl 1-^{13}C-Acetate 7b. To a round-bottom distillation flask (0.5 L) equipped with a magnetic stir bar, ruthenium(III) chloride hydrate (0.05 equiv, 16.4 mmol, 3.40 g), sodium 1-^{13}C-acetate (0.051 equiv, 16.7 mmol, 1.39 g, 98% isotopic purity), vinyl laurate (4 equiv, 1311 mmol, 341 mL), and 1-^{13}C-acetic acid (98.0 mmol, 20.00 g, 98% isotopic purity) were added. The reaction mixture was stirred at 35 °C overnight. The flask was attached to a distillation apparatus: three-way distillation connecting adapter with mercury thermometer on top, distillation condenser (water), distillation adapter with vacuum takeoff, and a round-bottom collection flask (25 mL). The system was put under argon atmosphere by temporarily replacing the thermometer with a rubber septum penetrated by a needle, which was connected to the argon gas line. We note that "vacuum takeoff" is used as gas exhaust during this procedure. After 0.5 h, the thermometer was quickly returned to its place and the vacuum takeoff was plugged with the rubber septum. Two needles (one connected to the argon line and the other one opened to atmosphere) were inserted into the septum. This setup keeps the system under inert gas, while avoiding pressure buildup. The collection flask was cooled in ice bath. The distillation flask was heated to 70 °C for 2 h. Then, the temperature was gradually increased to 220 °C using an oil bath. After 2 h, distillation was completed and crude vinyl 1-^{13}C-acetate was washed with 2 × 20 mL of saturated $NaHCO_3$ solution, with 2 × 20 mL of $NaHSO_3$ solution, and again with 20 mL of saturated $NaHCO_3$ solution and dried with anhydrous $CaCl_2$. The product was distilled under atmospheric pressure (bp 74 °C). The yield is 16.4 g (186 mmol, 55%) based on combined loading of sodium 1-^{13}C-acetate and 1-^{13}C-acetic acid.

^{1}H NMR (400 MHz, $CDCl_3$): 7.21−7.27 (m, 1H), 5.27 (dm, 1H, J = 17.2 Hz), 4.85 (d, 1H, J = 14.0 Hz), 4.54 (d, 1H, J = 6.2 Hz), 2.10 (d, 3H, J = 7.0 Hz). ^{13}C NMR (100 MHz, $CDCl_3$): 168.0, 141.3 (d, J = 2.4 Hz), 97.7 (d, J = 3.8 Hz), 20.7 (d, J = 60.6 Hz).

General Procedure P for the Synthesis of Allyl and Propargyl Pyruvates. Pyruvic acid (0.12 mol, 1 equiv), alcohol (1.2 equiv), p-TsOH (0.05 equiv), and 130 mL of benzene were mixed in a 250 mL round-bottom flask equipped with a Dean−Stark adapter and condenser. The apparatus was flushed with argon, and the reaction mixture was refluxed for 2−4 h until 1 equiv of water was collected in the trap of the Dean−Stark adapter. After cooling, the reaction mixture was washed with 2 × 100 mL of saturated $NaHCO_3$ solution and 2 × 100 mL of water and dried with anhydrous $CaCl_2$. Excess benzene was removed using a rotational evaporator under 25 °C, 50 Torr (65 mbar), and 120 rpm. The crude product was distilled under a reduced pressure of 30 Torr (40 mbar).

Allyl Pyruvate 8a. Allyl pyruvate **8a** was obtained using general procedure P from 10.0 g of pyruvic acid. The yield was 5.6 g (40%).

^{1}H NMR (400 MHz, $CDCl_3$): 5.93 (ddt, 1H, J = 17.2, 10.4, and 6.0 Hz), 5.37 (dm, 1H, J = 17.2 Hz), 5.29 (dm, 1H, J = 10.5 Hz), 4.70 (dm, 2H, J = 6.0 Hz), 2.44 (s, 3H). ^{13}C NMR (100 MHz, $CDCl_3$): 191.7, 160.5, 130.8, 120.1, 67.0, 26.8.

Propargyl Pyruvate 9a.[62] Propargyl pyruvate **9a** was obtained using general procedure P from 10.0 g of pyruvic acid. The yield was 3.8 g (30%).

^{1}H NMR (400 MHz, $CDCl_3$): 4.78 (dm, 2H, J = 2.2 Hz), 2.51 (tm, 1H, J = 2.2 Hz), 2.44 (s, 3H). ^{13}C NMR (100 MHz, $CDCl_3$): 190.7, 160.8, 76.3, 76.3, 53.6, 26.7.

Allyl 1-^{13}C-Pyruvate 8b. Allyl 1-^{13}C-pyruvate **8b** was obtained using general procedure P from 10.0 g of 1-^{13}C-pyruvic acid. The yield was 8.7 g (60%).

^{1}H NMR (400 MHz, $CDCl_3$): 5.87−5.97 (m, 1H), 5.36 (dm, 1H, J = 17.2 Hz), 5.27 (dm, 1H, J = 10.2 Hz), 4.68−4.71 (m, 2H), 2.42−2.44 (m, 3H). ^{13}C NMR (100 MHz, $CDCl_3$): 191.7 (d, J = 67.8 Hz), 160.5, 130.8 (d, J = 2.0 Hz), 120.0, 66.9 (d, J = 2.5 Hz), 26.8 (d, J = 16.8 Hz).

Propargyl 1-^{13}C-Pyruvate 9b. Propargyl 1-^{13}C-pyruvate **9b** was obtained using general procedure P from 10.0 g of 1-^{13}C-pyruvic acid. The yield was 4.8 g (35%).

^{1}H NMR (400 MHz, $CDCl_3$): 4.74−4.76 (m, 2H), 2.48−2.52 (m, 1H), 2.41 (s, 3H). ^{13}C NMR (100 MHz, $CDCl_3$): 190.7 (d, J = 67.4 Hz), 159.8, 76.3, 76.3, 53.5 (d, J = 2.5 Hz), 26.7 (d, J = 17.0 Hz).

Preparation Procedures for Vinyl Pyruvate 10a. To a round-bottom flask (1 L) equipped with a magnetic stir bar, palladium(II) acetate (0.2 equiv, 23 mmol, 5.0 g), potassium hydroxide (0.13 equiv, 15 mmol, 0.82 g), vinyl acetate (96 equiv, 10 849 mmol, 1000 mL), and pyruvic acid (113.0 mmol, 10.00 g) were added. The reaction mixture was stirred at 25 °C for 3 days. The mixture was filtered through a filter paper, and the residue was washed with vinyl acetate (100 mL). The organic layer was washed with 3 × 200 mL of saturated NaCl solution and 2 × 200 mL of saturated $NaHCO_3$ solution and dried with anhydrous $CaCl_2$. Excess vinyl acetate was removed using a rotational evaporator under 25 °C, 50 Torr (65 mbar), and 120 rpm. The crude product was distilled under a reduced pressure of 30 Torr (40 mbar). The yield was 0.8 g (6%).

^{1}H NMR (400 MHz, $CDCl_3$): 7.25 (dd, 1H, J = 13.8 and 6.2 Hz), 5.157 (dd, 1H, J = 13.8 and 2.2 Hz), 4.80 (dd, 1H, J = 10.5 Hz), 4.53 (dm, 2H, J = 6.2 and 2.2 Hz), 2.49 (s, 3H). ^{13}C NMR (100 MHz, $CDCl_3$): 190.6, 157.5, 140.7, 101.4, 26.76.

We note that the corresponding NMR spectra of the synthesized compounds are provided in the Supporting Information (SI).

Parahydrogen Production. Parahydrogen gas was produced using custom-built pH_2 generator based on cryocooler module (SunPower, P/N 100490, CryoTel GT). The cryocooler unit was cooled by a water chiller placed inside the generator chassis. The generator measures 18 in. (width), 26 in. (depth), and 33.5 in. (height) and has four casters allowing for relatively easy portability. This cryogen-free device produces up to 150 standard cubic centimeters per minute (150 sccm) of pH_2 at the temperature as low as 42 K and up to 500 psi (34 atm) H_2 pressure. For the work presented here, the generator was operated at 60−63 K, resulting in approximately 66−63% pH_2 fraction enrichment.

DOI: 10.1021/acsomega.8b00983
ACS Omega 2018, 3, 6673−6682

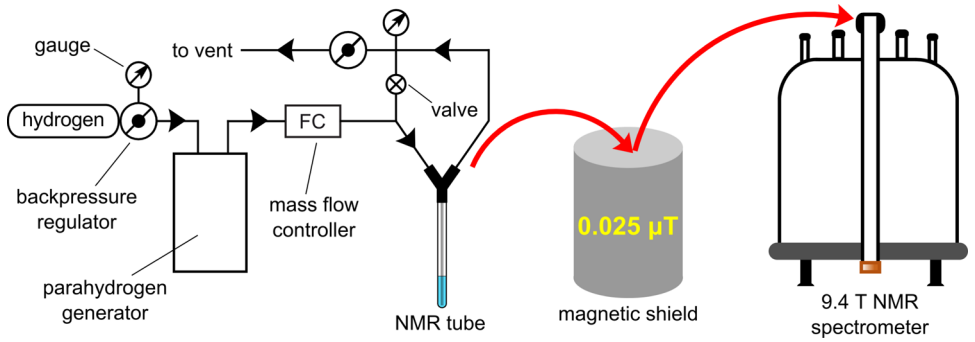

Figure 1. Experimental setup for PHIP-SAH hyperpolarization and NMR spectroscopic detection at 9.4 T. The safety valve indicated as ⌀ is set to 40 or 70 psig in the studies performed.

Preparation of Solution for ^{13}C PHIP-SAH Hyperpolarization. Commercially available bis(norbornadiene)-rhodium(I) tetrafluoroborate ($[Rh(NBD)_2]BF_4$, NBD = norbornadiene, Strem 45-0230), 1,4-bis(diphenylphosphino)-butane (dppb, Sigma-Aldrich, 98%), and ultrapure hydrogen (>99.999%) were used as received. The overall scheme of the experimental setup is presented in Figure 1. Hydrogen gas was enriched with pH_2 to 63−66% para-state using a homemade parahydrogen generator. pH_2 gas flow rate was regulated with a mass flow controller (SmartTrak 50, Sierra Instruments, Monterey, CA). Hydrogenation reactions were carried out in 5 mm NMR tubes tightly connected with 1/4 in. outer diameter poly(tetrafluoroethylene) tubes.

For hydrogenation in CD_3OD, the required amounts of $[Rh(NBD)_2]BF_4$ and dppb corresponding to 5 mM concentration and propargyl 1-^{13}C-pyruvate corresponding to 80 mM concentration were dissolved in CD_3OD under argon atmosphere and mixed using a vortex mixer. Standard Wilmad NMR tubes were filled with 0.7 mL of resultant solution under argon atmosphere, preheated up to 40 °C inside the NMR spectrometer, and pressurized with parahydrogen up to 40 psig. The pH_2 was bubbled for 10 s at a 40 standard cubic centimeters per minute (sccm) flow rate and a 40 psig pressure.

For hydrogenation in D_2O, a previously described procedure[32] was employed for the preparation of aqueous catalyst solution (~5.3 mM concentration) in D_2O. Unsaturated PHIP precursor was added resulting in ~80 mM concentration. Medium-wall 5 mm NMR tubes (Wilmad glass P/N 503-PS-9) were filled with 0.5 mL of resultant solution under argon atmosphere, preheated up to 85 °C in hot water, and pressurized with pH_2 up to 70 psig (Figure 1). The pH_2 was bubbled for 30 s at a 140 sccm flow rate and a 70 psig pressure.

After termination of hydrogen bubbling, the samples were placed inside the MuMETAL magnetic shield described in detail in ref 56. The magnetic field inside the shield was adjusted to ~0.025 μT using additional solenoid placed inside the previously degaussed three-layered MuMETAL shield (Magnetic Shield Corp., Bensenville, IL, P/N ZG-206). This previously calibrated solenoid was powered by a direct current (DC) power supply (GW-Instek, GPR-30600), and the DC current was attenuated by a resistor bank (Global Specialties, RDB-10) to achieve the desired magnetic field inside the MuMETAL shield. This exact setup with adjustable magnetic field was previously employed for hyperpolarization experiments using signal amplification by reversible exchange.[63−65] Then, the samples were slowly (~1 s) pulled out of the shield and placed inside the probe of 9.4 T Bruker NMR spectrometer for detection or transferred to the radiofrequency (rf) coil of a 15.2 T MRI scanner. PHIP NMR spectra were acquired as pseudo-two-dimensional (2D) sets consisting of 64 ^{1}C NMR spectra (acquisition time, ~1 s) to avoid delays between placing the sample into the probe and starting of the acquisition. The acquisition always started before placing the sample inside the NMR probe, and the first spectra containing signal were used for presentation here. All NMR spectra were acquired using 90° rf pulse. The sample transfer time from the shield to NMR spectrometer was approximately 8 s. The sample transfer time to MRI scanner was approximately 20 s.

RESULTS AND DISCUSSION

General Considerations. There are certain requirements to the structure of the molecule for the hyperpolarization of substrates by the PHIP method. The substrate must contain an unsaturated (double C═C or triple C≡C) carbon−carbon bond for subsequent pH_2 pairwise addition. Moreover, isotopic labeling of PHIP precursors with ^{13}C is required to boost the payload of ^{13}C hyperpolarization from natural abundance of ^{13}C (~1.1%) to ~99%.[5] Moreover, the PHIP-SAH approach requires a spin−spin (J) coupling network between the enriched ^{13}C site and the nascent parahydrogen-derived protons (Scheme 1).[10,33,34,36,53] In the context of PHIP-SAH technique and the precursors of interest studied here (i.e., acetate and pyruvate), carboxyl carbon is enriched with ^{13}C because it has the longest ^{13}C T_1, which is advantageous from the perspective of biomedical application.[5] The network of spin−spin couplings is established with nascent pH_2-derived protons after their pairwise addition into the ester moiety.[36,53] The goal of this work is the synthesis of unsaturated esters with ^{13}C-labeled carboxyl sites employing biocompatible carboxylic acids, such as acetic acids (**1a**, **1b**), pyruvic acids (**2a**, **2b**), unsaturated allyl alcohol (**3**), and propargyl alcohol (**4**).

Synthesis of PHIP-SAH Precursors. Acetic acid esters **5a**, **5b**, and **6a**, **6b** were obtained by the reaction of acetic acid **1a** or labeled 1-^{13}C-acetic acid **1b** with a small excess of allyl alcohol **3** or propargyl alcohol **4** in the presence of *p*-toluenesulfonic acid (Scheme 3). All reactions were refluxed with the Dean−Stark adapter without any additional solvent. Approximately 1 equiv of water was collected in the trap of the Dean−Stark adapter for 4−8 h. Products **5a**, **5b**, and **6a**, **6b** were distilled under atmospheric pressure for final purification with the yield of 45−75% (Table 1). Although these compounds have been synthesized and characterized in the unlabeled forms **5a** and **6a** previously,[66,67] the syntheses of

DOI: 10.1021/acsomega.8b00983
ACS Omega 2018, 3, 6673−6682

Scheme 3. Synthesis of Allyl and Propargyl Acetates[a]

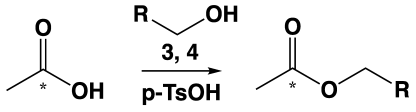

1a: acetic acid
1b: 1-^{13}C-acetic acid
3: prop-2-en-1-ol, R = -CH=CH$_2$
4: prop-2-yn-1-ol, R = -C≡CH

5a, 5b, 6a, 6b

[a]Note: the asterisk symbol denotes the optional labeling with ^{13}C isotope.

Table 1. Reaction Yields for All Synthesized Substrates (5−10)

reagent/source of ^{13}C label	product/PHIP precursor	yield (%)
acetic acid **1a**	allyl acetate **5a**	75
acetic acid **1a**	propargyl acetate **6a**	45
1-^{13}C-acetic acid **1b**	allyl 1-^{13}C-acetate **5b**	70
1-^{13}C-acetic acid **1b**	propargyl 1-^{13}C-acetate **6b**	45
1-^{13}C-acetic acid **1b**	vinyl 1-^{13}C-acetate **7b**	55
pyruvic acid **2a**	allyl pyruvate **8a**	40
pyruvic acid **2a**	propargyl pyruvate **9a**	30
1-^{13}C-pyruvic acid **2b**	allyl 1-^{13}C-pyruvate **8b**	60
1-^{13}C-pyruvic acid **2b**	propargyl 1-^{13}C-pyruvate **9b**	35
pyruvic acid **2a**	vinyl pyruvate **10a**	6

these labeled variants **5b** and **6b** have been reported here for the first time to the best of our knowledge. We note that the preparation of pure from the solvent PHIP-SAH precursor compounds is required for PHIP hyperpolarization because the presence of organic solvent is undesirable for in vivo studies and prohibitive for future human use.

Pyruvic acid esters **8a**, **8b**, and **9a**,[62] **9b** were obtained by the reaction of pyruvic acid **2a** or labeled 1-^{13}C-pyruvic acid **2b** with small excess of allyl alcohol **3** or propargyl alcohol **4** in the presence of a *p*-toluenesulfonic acid (Scheme 4). All reactions

Scheme 4. Synthesis of Allyl and Propargyl Pyruvates[a]

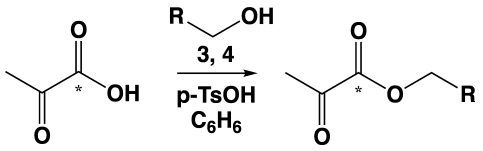

2a: pyruvic acid
2b: 1-^{13}C-pyruvic acid
3: prop-2-en-1-ol, R = -CH=CH$_2$
4: prop-2-yn-1-ol, R = -C≡CH

8a, 8b, 9a, 9b

[a]Note: the asterisk symbol denotes the optional labeling with ^{13}C isotope.

were refluxed with the Dean−Stark adapter with benzene as a solvent. Water (1 equiv) was collected in the trap of the Dean−Stark adapter for 2−4 h (the use of the Dean−Stark apparatus was required to remove water to prepare pure compounds because water can form azeotrope mixtures with esters, including those studied here). Products **8a**, **8b**, and **9a**, **9b** were distilled under reduced pressure (30 Torr) for final purification with the yield of 30−60% (Table 1). Although these compounds have been synthesized in the unlabeled form **8a** and **9a** previously,[62,68] the syntheses of these labeled variants **8b** and **9b** have been reported here for the first time to the best of our knowledge. Moreover, we report the preparation of pure (from organic solvent) compounds, which is desirable for PHIP-SAH hyperpolarization. We also note that the overall yields for compounds **9a** and **9b** were lower than those previously reported for **9a**[62] because here neat liquid (vs solutions) was prepared as the final product. The additional achievement of the reported work is the synthesis of ^{13}C-labeled compounds in pure form.

We note that during preparation of this manuscript, Cavallari and co-workers[55] reported on a study of PHIP-SAH, where they employed **9b** (i.e., isotopically enriched propargyl pyruvate). However, the detailed synthesis of **9b** was not reported in ref 55, instead they stated that they have employed previously published procedure for the preparation of propargyl 1-^{13}C-lactate with ∼15% overall yield.[54] The procedure reported here is more than 2-fold efficient with the overall yield of ∼35% (Table 1). Moreover, to the best of our knowledge, our work provides synthetic details for the preparation of propargyl 1-^{13}C-pyruvate for the first time.

The yield difference in case of labeled versus nonlabeled compounds is due to a combination of run-to-run reproducibility and purity of initial ^{13}C reagent. This yield difference is the most pronounced for compounds **8a** and **8b** (Table 1).

Synthesis of vinyl 1-^{13}C-acetate **7b** was described previously from 1-^{13}C-acetic acid **1b** and vinyl laurate **11** (Scheme 5).[56]

Scheme 5. Synthesis of Vinyl 1-^{13}C-Acetate 7b[a]

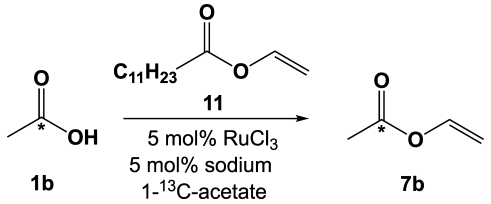

1b **7b**

[a]Note: the asterisk symbol denotes the optional labeling with ^{13}C isotope.

We carried out large-scale synthesis (20 g of **1b**) and developed a method of purification of product. The main impurity was acetaldehyde, which was removed by washing with an aqueous solution of sodium bisulfate. The total yield of pure **10b** was 55% (Table 1). We note that the procedure reported here has nearly doubled the yield (55 vs 31% reported previously) and more than doubled the scale (with nearly 4-fold increase of the final product).[56]

The same approach used for the preparation of vinyl acetate has failed for the synthesis of vinyl pyruvate from pyruvic acid **2a**. There was no reaction according to NMR spectra of reaction mixture even under reflux. Cavallari and co-workers obtained vinyl lactate using transvinylation by $Pd(OAc)_2$.[54] We achieved only 6% (Table 1) of the yield for vinyl pyruvate **10a** using this procedure (Scheme 6) after distillation under reduced pressure. To the best of our knowledge, this study is the first report of preparation of vinyl pyruvate in the nonlabeled (i.e., at natural abundance of isotopes) form from pyruvic acid (although synthesis from other starting material was reported,[69] it is not readily suitable for ^{13}C enrichment using 1-^{13}C-pyruvic acid as the source of ^{13}C spin label). We note that vinyl pyruvate can exist in acetalic form in methanol, which is evident from the corresponding NMR spectra provided in the SI (the presence of other additional proton

DOI: 10.1021/acsomega.8b00983
ACS Omega 2018, 3, 6673−6682

Scheme 6. Synthesis of Vinyl Pyruvate 10a[a]

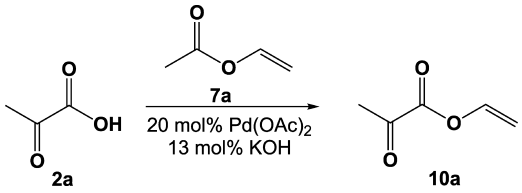

[a]Note: the labeling with ^{13}C isotope was not tested due to significantly lower yield (~6%) and significantly higher cost (10-fold) of 1-^{13}C-pyruvic acid compared to 1-^{13}C-acetic acid (see Table 1 for details).

NMR peaks about 1−3 ppm and ^{13}C NMR signals of vinyl carbons can likely be explained by the existence of various conformers of the CH_2═CH−O−C═O moiety).

Feasibility of ^{13}C PHIP-SAH Hyperpolarization. The feasibility of PHIP-SAH hyperpolarization has been demonstrated for several substrates in the past, including pyruvate moiety in unlabeled form.[36,53−58,70] Here, we demonstrate PHIP-SAH using 1-^{13}C-enriched pyruvate (the most interesting moiety) because of its ubiquitous place in metabolic pathways, which are upregulated in cancer[13,14,71,72] and many other diseases and disorders.[6,8,17,73,74] We note that isotopic ^{13}C enrichment is required for in vivo bioimaging applications to provide the additional sensitivity boost by ~90-fold compared to the use of nonisotopically enriched compounds. PHIP-SAH hyperpolarization performed in a 5 mm NMR tube was analyzed via ^{13}C spectroscopy at 9.4 T (Figures 2 and 3). When the HP product was detected at 9.4 T, the ^{13}C signal was enhanced by ~4100-fold in CD_3OD solution corresponding to ^{13}C polarization of ~3.2% (Figure 2b). In case of PHIP-SAH in aqueous medium, the signal enhancement (SE) and ^{13}C polarization were approximately 4-fold lower: SE of ~970 corresponding to ^{13}C polarization of ~0.7% (Figure 3b). The SE values were calculated by comparing HP spectra to thermally polarized spectra (Figures 2c and 3c, respectively). ^{13}C polarization was calculated by multiplying the SE values by ^{13}C thermal polarization at 25 °C and 9.4 T.

The lower ^{13}C polarization values in D_2O versus those in CD_3OD are not surprising because hydrogen solubility in aqueous medium is approximately an order of magnitude lower than that in methanol.[75−79] This fact leads to lower hydrogenation reaction rates and greater polarization losses during pH_2 bubbling step (note: pH_2 bubbling was 10 s in case of CD_3OD and 30 s in case of D_2O solvent). While the relaxation of nascent pH_2-derived protons was not studied here, the previous low-field relaxation studies in HP ethyl acetate motif (T_1 of ~7.2 s in methanol and ~4.3 s in water)[80] indeed support the hypothesis that a significant fraction of pH_2-derived hyperpolarization decays during 10 s bubbling in methanol. This effect is further exacerbated in water, where bubbling occurred for 3 times longer period of time and at higher relaxation rates. We note that polarization losses are not taken into account for both hyperpolarization approaches in CD_3OD and D_2O during ~8 s long sample transfer procedure. We also note that optimization of percentage of achieved ^{13}C polarization was not the main goal of this work, although future studies to improve percentage polarization are certainly warranted. The use of higher-pressure setups[81] and high-pressure reaction chambers with spray injection[50,61,82−84] will likely increase hydrogenation rates and will effectively lead to

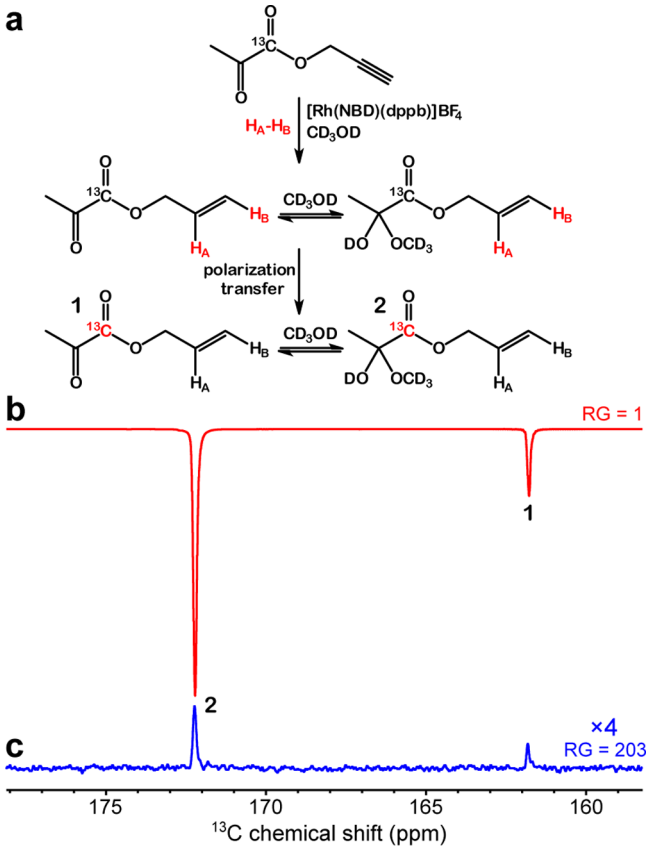

Figure 2. (a) Reaction scheme of propargyl 1-^{13}C-pyruvate hydrogenation with pH_2 over [Rh(NBD)(dppb)]BF_4 complex in CD_3OD solution with subsequent polarization transfer from protons to ^{13}C. (b) ^{13}C NMR spectrum of HP allyl 1-^{13}C-pyruvate in CD_3OD and (c) the corresponding ^{13}C NMR spectrum of reaction mixture after relaxation of hyperpolarization (thermal spectrum). Spectrum (b) was acquired with receiver gain (RG) = 1 due to very high polarization leading to signal overflow at higher RG values. In CD_3OD, signal enhancement (SE) was ~4100, corresponding to ^{13}C polarization of ~3.2%. Note: the linear receiver gain (RG) was used for spectra acquisition.

significantly higher polarization levels due to decreased polarization losses. Moreover, the use of ~100% pH_2 versus ~66% employed here would nearly double the ^{13}C polarization values. On the basis of the previous work of ours[50,56] and others,[36,55] ^{13}C polarization levels in excess of 20% may be feasible using this PHIP-SAH approach, including 1-^{13}C-pyruvate derivative studied here.

Figures 2a and 3a describe the chemical conversion during the PHIP-SAH hyperpolarization process. We note that the reversible addition of solvent molecule to carbonyl group of allyl 1-^{13}C-pyruvate leads to the fact that the hydrogenation product is present in the form of two species manifesting themselves as two HP and thermally polarized resonances in all ^{13}C spectra shown in Figures 2 and 3.

Feasibility of ^{13}C PHIP-SAH MRI Imaging Using ^{13}C Hyperpolarized Pyruvate. The produced aqueous HP allyl 1-^{13}C-pyruvate (see above) solution was imaged using a Bruker 15.2 T small-animal MRI scanner employing ^{13}C surface rf coil. The HP liquid (aqueous liquid containing 80 mM ^{13}C substrate) was injected into a ~2.8 mL hollow sphere via a catheter (simulating future in vivo experimentations), and 2D projection ^{13}C images were recorded (Figure 4a). The

DOI: 10.1021/acsomega.8b00983
ACS Omega 2018, 3, 6673−6682

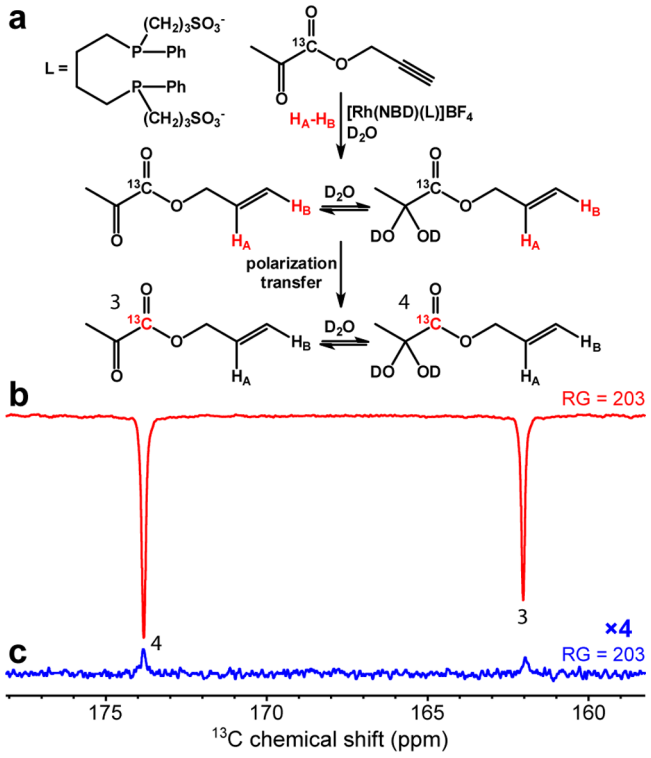

Figure 3. (a) Reaction scheme of propargyl 1-^{13}C-pyruvate hydrogenation with pH_2 over water-soluble rhodium complex in D_2O solution with subsequent polarization transfer from protons to ^{13}C. (b) ^{13}C NMR spectrum of HP allyl 1-^{13}C-pyruvate in D_2O and (c) the corresponding ^{13}C NMR spectrum of reaction mixture after relaxation of hyperpolarization. Both NMR spectra were acquired with RG = 203. In D_2O, signal enhancement (SE) was ~970, corresponding to ^{13}C polarization of ~0.7%. Note: the linear receiver gain (RG) was used for spectra acquisition.

corresponding ^{13}C image of thermally polarized concentrated sodium 1-^{13}C-acetate is shown in Figure 4b.

Both samples for imaging were placed above the rf coil. We note that because surface rf coil was used, it had poor penetration in the sample. As a result, the top part of the sphere imaged in Figure 4b exhibits a significantly reduced intensity. The maximum signal-to-noise ratio (SNR) in HP image was 33, and the maximum SNR of thermally polarized sample was 91 (note the different size voxel in the images; the SNR was not corrected for the difference in the voxel size). We note that the image in Figure 4a visualizes a partially filled sphere and that the meniscus of the HP liquid is clearly delineated. The apparent "ghosting" (seen as two overlapping half-circles) is due to the presence of two HP ^{13}C resonances with nearly equal signal intensities (Figure 3b). As a result, the MRI image encoding (in 2D trueFISP (Bruker ParaVision 5.1) sequence) in the frequency domain leads to an apparent shift (by a few pixels) of these two species in the ^{13}C MRI image in Figure 4a. The corresponding thermal image after the decay of HP state in Figure 4a was recorded (data not shown), and it revealed only noise. To the best of our knowledge, Figure 4a is one of the first reports of ^{13}C MRI image of HP 1-^{13}C-pyruvate moiety produced via PHIP hyperpolarization technique.

While d-DNP has reported record levels of ^{13}C polarization for 1-^{13}C-pyruvate ($\%P_{13C}$ ~ 60%[85]) and 1-^{13}C-acetate ($\%P_{13C}$ > 35%[86]) moieties, d-DNP is significantly a more instrumentationally demanding technique requiring cryogenic high-field equipment and a significantly more costlier technique (~$10^6) compared to PHIP hyperpolarization technique (<$10^5). The detailed analysis is provided in a recent review by Hövener and co-workers.[5] While only $\%P_{13C}$ of ~3.2% was demonstrated here for 1-^{13}C-pyruvate moiety in this report (although Cavallari and co-workers have recently demonstrated $\%P_{13C}$ of ~5%[55]), future optimization of PHIP-SAH polarization process and the use of high-pressure spray injection hyperpolarizer may significantly increase $\%P_{13C}$ to above 20%;[36] for

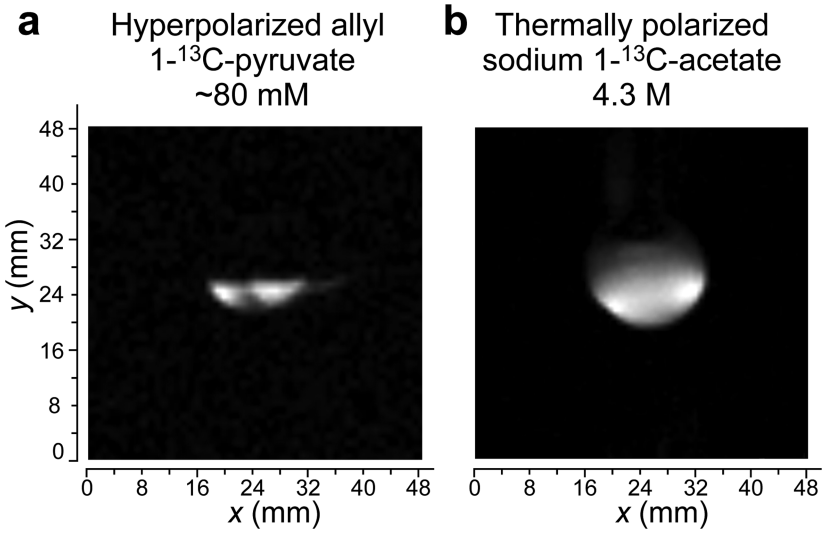

Figure 4. Two-dimensional trueFISP MRI image of aqueous HP allyl 1-^{13}C-pyruvate (a) and thermally polarized sodium 1-^{13}C-acetate (b) employed for referencing purposes. In (a), the solution is injected into a partially filled hollow 2.8 mL plastic sphere (rf coil is under the phantom). In (b), the solution is filled in a 2.8 mL hollow plastic sphere (rf coil is under the phantom). Imaging parameters: repetition time = 4.8 ms; echo time = 2.4 ms; total acquisition time = ~0.3 s; imaging matrix = 64 × 64; field of view = 64 × 64 mm^2 (a), 48 × 48 mm^2 (b); pixel size = 1 × 1 mm^2 (a), 0.75 × 0.75 mm^2 (b). Note: slightly different imaging parameters for the thermally polarized phantom and HP material: the signal-to-noise ratio (SNR) is not corrected for the different size voxel in these two images. The excitation rf pulse angle for the surface coil was optimized on thermally polarized 1-^{13}C-acetate sample to maximize SNR.

DOI: 10.1021/acsomega.8b00983
ACS Omega 2018, 3, 6673−6682

example, $\%P_{13C}$ of >25%[50] was reported for HP 1-^{13}C-succinate using PHIP hyperpolarizer. Values of $\%P_{13C}$ above 20% will render the solutions usable for in vivo use in a manner similar to d-DNP technique,[6] but at significantly lower instrumentation and operation costs and at a significantly shorter production times, i.e., ∼1 min versus ∼1 h by d-DNP.[5]

CONCLUSIONS

In conclusion, systematic synthetic preparation of 1-[^{13}C] isotopically enriched acetates and pyruvates derivatized with unsaturated ester moiety is reported. Vinyl 1-^{13}C-acetate (55% yield), allyl 1-^{13}C-acetate (70% yield), propargyl 1-^{13}C-acetate (45% yield), allyl 1-^{13}C-pyruvate (60% yield), and propargyl 1-^{13}C-pyruvate (35% yield) were prepared on a comparatively large (multigram) scale. The reported high yields will be useful for future preparation, in vivo validation, and clinical trials of molecular imaging employing injectable HP 1-^{13}C-acetate and 1-^{13}C-pyruvate derivatives. The yield of vinyl pyruvate was significantly lower (6%), and the reported approach was deemed nonefficient for the preparation of the 1-^{13}C-labeled variant. The synthesized compounds were sufficiently pure for PHIP-SAH feasibility demonstration: HP allyl 1-^{13}C-pyruvate from propargyl 1-^{13}C-pyruvate with ^{13}C polarization of ∼3.2% in CD_3OD and ∼0.7% in D_2O was produced. ^{13}C MRI imaging of HP 1-^{13}C-pyruvate was demonstrated in D_2O medium.

ASSOCIATED CONTENT

Supporting Information

The Supporting Information is available free of charge on the ACS Publications website at DOI: 10.1021/acsomega.8b00983.

NMR spectra and other supporting figures (PDF)

AUTHOR INFORMATION

Corresponding Author

*E-mail: chekmenev@wayne.edu.

ORCID

Kirill V. Kovtunov: 0000-0001-7577-9619

Igor V. Koptyug: 0000-0003-3480-7649

Eduard Y. Chekmenev: 0000-0002-8745-8801

Notes

The authors declare no competing financial interest.

ACKNOWLEDGMENTS

N.V.C, O.G.S., and K.V.K. acknowledge the Russian Foundation for Basic Research and the government of the Novosibirsk region of the Russian Federation (grant 18-43-543023 p_mol_a) for the support of the molecules synthesis and their testing with parahydrogen. I.V.K. acknowledges the Federal Agency for Scientific Organizations #0333-2017-0002 for the support of the studies of H_2 activation. MRI studies were supported by NSF CHE-1416268 and CHE-1416432, NIH 1R21EB020323 and R21CA220137, and DOD CDMRP BRP W81XWH-12-1-0159/BC112431, and RFBR (17-54-33037-OHKO_a, 16-03-00407_a). The authors thank Dr. Isaac V. Manzanera Esteve for assistance with imaging studies.

REFERENCES

(1) Goodson, B. M.; Whiting, N.; Coffey, A. M.; Nikolaou, P.; Shi, F.; Gust, B. M.; Gemeinhardt, M. E.; Shchepin, R. V.; Skinner, J. G.; Birchall, J. R.; et al. Hyperpolarization Methods for MRS. *eMagRes* **2015**, *4*, 797−810.

(2) Nikolaou, P.; Goodson, B. M.; Chekmenev, E. Y. NMR Hyperpolarization Techniques for Biomedicine. *Chem. − Eur. J.* **2015**, *21*, 3156−3166.

(3) Barskiy, D. A.; Coffey, A. M.; Nikolaou, P.; Mikhaylov, D. M.; Goodson, B. M.; Branca, R. T.; Lu, G. J.; Shapiro, M. G.; Telkki, V.-V.; Zhivonitko, V. V.; et al. NMR Hyperpolarization Techniques of Gases. *Chem. − Eur. J.* **2017**, *23*, 725−751.

(4) Duckett, S. B.; Mewis, R. E. Application of Parahydrogen Induced Polarization Techniques in NMR Spectroscopy and Imaging. *Acc. Chem. Res.* **2012**, *45*, 1247−1257.

(5) Hövener, J.-B.; Pravdivtsev, A. N.; Kidd, B.; Bowers, C. R.; Glöggler, S.; Kovtunov, K. V.; Plaumann, M.; Katz-Brull, R.; Buckenmaier, K.; Jerschow, A.; et al. Parahydrogen-Based Hyperpolarization for Biomedicine. *Angew. Chem., Int. Ed.* **2018**, DOI: 10.1002/anie.201711842.

(6) Kurhanewicz, J.; Vigneron, D. B.; Brindle, K.; Chekmenev, E. Y.; Comment, A.; Cunningham, C. H.; DeBerardinis, R. J.; Green, G. G.; Leach, M. O.; Rajan, S. S.; et al. Analysis of Cancer Metabolism by Imaging Hyperpolarized Nuclei: Prospects for Translation to Clinical Research. *Neoplasia* **2011**, *13*, 81−97.

(7) Brindle, K. M. Imaging Metabolism with Hyperpolarized ^{13}C-Labeled Cell Substrates. *J. Am. Chem. Soc.* **2015**, *137*, 6418−6427.

(8) Golman, K.; in't Zandt, R.; Thaning, M. Real-Time Metabolic Imaging. *Proc. Natl. Acad. Sci. U.S.A.* **2006**, *103*, 11270−11275.

(9) Gallagher, F. A.; Kettunen, M. I.; Day, S. E.; Hu, D. E.; Ardenkjaer-Larsen, J. H.; in't Zandt, R.; Jensen, P. R.; Karlsson, M.; Golman, K.; Lerche, M. H.; et al. Magnetic Resonance Imaging of pH in Vivo Using Hyperpolarized C-13-Labelled Bicarbonate. *Nature* **2008**, *453*, 940−943.

(10) Goldman, M.; Johannesson, H.; Axelsson, O.; Karlsson, M. Hyperpolarization of C-13 through Order Transfer from Parahydrogen: A New Contrast Agent for MFI. *Magn. Reson. Imaging* **2005**, *23*, 153−157.

(11) Golman, K.; Axelsson, O.; Johannesson, H.; Mansson, S.; Olofsson, C.; Petersson, J. S. Parahydrogen-Induced Polarization in Imaging: Subsecond C-13 Angiography. *Magn. Reson. Med.* **2001**, *46*, 1−5.

(12) Ardenkjaer-Larsen, J. H.; Fridlund, B.; Gram, A.; Hansson, G.; Hansson, L.; Lerche, M. H.; Servin, R.; Thaning, M.; Golman, K. Increase in Signal-to-Noise Ratio of >10,000 Times in Liquid-State NMR. *Proc. Natl. Acad. Sci. U.S.A.* **2003**, *100*, 10158−10163.

(13) Albers, M. J.; Bok, R.; Chen, A. P.; Cunningham, C. H.; Zierhut, M. L.; Zhang, V. Y.; Kohler, S. J.; Tropp, J.; Hurd, R. E.; Yen, Y.-F.; et al. Hyperpolarized C-13 Lactate, Pyruvate, and Alanine: Noninvasive Biomarkers for Prostate Cancer Detection and Grading. *Cancer Res.* **2008**, *68*, 8607−8615.

(14) Day, S. E.; Kettunen, M. I.; Gallagher, F. A.; Hu, D. E.; Lerche, M.; Wolber, J.; Golman, K.; Ardenkjaer-Larsen, J. H.; Brindle, K. M. Detecting Tumor Response to Treatment Using Hyperpolarized C-13 Magnetic Resonance Imaging and Spectroscopy. *Nat. Med.* **2007**, *13*, 1382−1387.

(15) Yen, Y. F.; Kohler, S. J.; Chen, A. P.; Tropp, J.; Bok, R.; Wolber, J.; Albers, M. J.; Gram, K. A.; Zierhut, M. L.; Park, I.; et al. Imaging Considerations for in Vivo C-13 Metabolic Mapping Using Hyperpolarized C-13-Pyruvate. *Magn. Reson. Med.* **2009**, *62*, 1−10.

(16) Comment, A.; Merritt, M. E. Hyperpolarized Magnetic Resonance as a Sensitive Detector of Metabolic Function. *Biochemistry* **2014**, *53*, 7333−7357.

(17) Merritt, M. E.; Harrison, C.; Storey, C.; Jeffrey, F.; Sherry, A.; Malloy, C. Hyperpolarized C-13 Allows a Direct Measure of Flux through a Single Enzyme-Catalyzed Step by NMR. *Proc. Natl. Acad. Sci. U.S.A.* **2007**, *104*, 19773−19777.

(18) Hurd, R. E.; Yen, Y.-F.; Mayer, D.; Chen, A.; Wilson, D.; Kohler, S.; Bok, R.; Vigneron, D.; Kurhanewicz, J.; Tropp, J.; et al. Metabolic Imaging in the Anesthetized Rat Brain Using Hyperpolarized 1-C-13 Pyruvate and 1-C-13 Ethyl Pyruvate. *Magn. Reson. Med.* **2010**, *63*, 1137−1143.

DOI: 10.1021/acsomega.8b00983
ACS Omega 2018, 3, 6673−6682

(19) Nelson, S. J.; Kurhanewicz, J.; Vigneron, D. B.; Larson, P. E. Z.; Harzstark, A. L.; Ferrone, M.; van Criekinge, M.; Chang, J. W.; Bok, R.; Park, I.; et al. Metabolic Imaging of Patients with Prostate Cancer Using Hyperpolarized 1-C-13 Pyruvate. *Sci. Transl. Med.* **2013**, *5*, No. 198ra108.
(20) Lai, M.; Gruetter, R.; Lanz, B. Progress Towards In vivo Brain ^{13}C-MRS in Mice: Metabolic Flux Analysis in Small Tissue Volumes. *Anal. Biochem.* **2017**, *529*, 229−244.
(21) Morris, P.; Bachelard, H. Reflections on the Application of ^{13}C-MRS to Research on Brain Metabolism. *NMR Biomed.* **2003**, *16*, 303−312.
(22) Befroy, D. E.; Perry, R. J.; Jain, N.; Dufour, S.; Cline, G. W.; Trimmer, J.; Brosnan, J.; Rothman, D. L.; Petersen, K. F.; Shulman, G. I. Direct Assessment of Hepatic Mitochondrial Oxidative and Anaplerotic Fluxes in Humans Using Dynamic ^{13}C Magnetic Resonance Spectroscopy. *Nat. Med.* **2014**, *20*, 98−102.
(23) Petersen, K. F.; Befroy, D. E.; Dufour, S.; Rothman, D. L.; Shulman, G. I. Direct Assessment of Hepatic Mitochondrial Oxidation and Pyruvate Cycling in Non Alcoholic Fatty Liver Disease by ^{13}C Magnetic Resonance Spectroscopy. *Cell Metab.* **2016**, *24*, 167−171.
(24) Mishkovsky, M.; Comment, A.; Gruetter, R. In Vivo Detection of Brain Krebs Cycle Intermediate by Hyperpolarized Magnetic Resonance. *J. Cereb. Blood Flow Metab.* **2012**, *32*, 2108−2113.
(25) Jensen, P. R.; Peitersen, T.; Karlsson, M.; in't Zandt, R.; Gisselsson, A.; Hansson, G.; Meier, S.; Lerche, M. H. Tissue-Specific Short Chain Fatty Acid Metabolism and Slow Metabolic Recovery after Ischemia from Hyperpolarized NMR in Vivo. *J. Biol. Chem.* **2009**, *284*, 36077−36082.
(26) Ardenkjaer-Larsen, J. H. On the Present and Future of Dissolution-DNP. *J. Magn. Reson.* **2016**, *264*, 3−12.
(27) Abragam, A.; Goldman, M. Principles of Dynamic Nuclear Polarization. *Rep. Prog. Phys.* **1978**, *41*, 395−467.
(28) Bowers, C. R.; Weitekamp, D. P. Transformation of Symmetrization Order to Nuclear-Spin Magnetization by Chemical-Reaction and Nuclear-Magnetic-Resonance. *Phys. Rev. Lett.* **1986**, *57*, 2645−2648.
(29) Bowers, C. R.; Weitekamp, D. P. Para-Hydrogen and Synthesis Allow Dramatically Enhanced Nuclear Alignment. *J. Am. Chem. Soc.* **1987**, *109*, 5541−5542.
(30) Bowers, C. R. Sensitivity Enhancement Utilizing Parahydrogen. In *eMagRes*; John Wiley & Sons, Ltd.: New York, 2007; pp 1−20.
(31) Eisenschmid, T. C.; Kirss, R. U.; Deutsch, P. P.; Hommeltoft, S. I.; Eisenberg, R.; Bargon, J.; Lawler, R. G.; Balch, A. L. Para Hydrogen Induced Polarization in Hydrogenation Reactions. *J. Am. Chem. Soc.* **1987**, *109*, 8089−8091.
(32) Cai, C.; Coffey, A. M.; Shchepin, R. V.; Chekmenev, E. Y.; Waddell, K. W. Efficient Transformation of Parahydrogen Spin Order into Heteronuclear Magnetization. *J. Phys. Chem. B* **2013**, *117*, 1219−1224.
(33) Goldman, M.; Johannesson, H. Conversion of a Proton Pair Para Order into C-13 Polarization by RF Irradiation, for Use in MRI. *C. R. Phys.* **2005**, *6*, 575−581.
(34) Goldman, M.; Johannesson, H.; Axelsson, O.; Karlsson, M. Design and Implementation of C-13 Hyperpolarization from Para-Hydrogen, for New MRI Contrast Agents. *C. R. Chim.* **2006**, *9*, 357−363.
(35) Bär, S.; Lange, T.; Leibfritz, D.; Hennig, J.; von Elverfeldt, D.; Hövener, J.-B. On the Spin Order Transfer from Parahydrogen to Another Nucleus. *J. Magn. Reson.* **2012**, *225*, 25−35.
(36) Cavallari, E.; Carrera, C.; Boi, T.; Aime, S.; Reineri, F. Effects of Magnetic Field Cycle on the Polarization Transfer from Parahydrogen to Heteronuclei through Long-Range J-Couplings. *J. Phys. Chem. B* **2015**, *119*, 10035−10041.
(37) Reineri, F.; Santelia, D.; Viale, A.; Cerutti, E.; Poggi, L.; Tichy, T.; Premkumar, S. S. D.; Gobetto, R.; Aime, S. Para-Hydrogenated Glucose Derivatives as Potential C-13-Hyperpolarized Probes for Magnetic Resonance Imaging. *J. Am. Chem. Soc.* **2010**, *132*, 7186−7193.
(38) Reineri, F.; Viale, A.; Ellena, S.; Boi, T.; Daniele, V.; Gobetto, R.; Aime, S. Use of Labile Precursors for the Generation of Hyperpolarized Molecules from Hydrogenation with Parahydrogen and Aqueous-Phase Extraction. *Angew. Chem., Int. Ed.* **2011**, *50*, 7350−7353.
(39) Reineri, F.; Viale, A.; Ellena, S.; Alberti, D.; Boi, T.; Giovenzana, G. B.; Gobetto, R.; Premkumar, S. S. D.; Aime, S. N-15 Magnetic Resonance Hyperpolarization Via the Reaction of Parahydrogen with N-15-Propargylcholine. *J. Am. Chem. Soc.* **2012**, *134*, 11146−11152.
(40) Bhattacharya, P.; Harris, K.; Lin, A. P.; Mansson, M.; Norton, V. A.; Perman, W. H.; Weitekamp, D. P.; Ross, B. D. Ultra-Fast Three Dimensional Imaging of Hyperpolarized C-13 in Vivo. *Magn. Reson. Mater. Phys., Biol. Med.* **2005**, *18*, 245−256.
(41) Bhattacharya, P.; Chekmenev, E. Y.; Perman, W. H.; Harris, K. C.; Lin, A. P.; Norton, V. A.; Tan, C. T.; Ross, B. D.; Weitekamp, D. P. Towards Hyperpolarized ^{13}C-Succinate Imaging of Brain Cancer. *J. Magn. Reson.* **2007**, *186*, 150−155.
(42) Chekmenev, E. Y.; Chow, S. K.; Tofan, D.; Weitekamp, D. P.; Ross, B. D.; Bhattacharya, P. Fluorine-19 NMR Chemical Shift Probes Molecular Binding to Lipid Membranes. *J. Phys. Chem. B* **2008**, *112*, 6285−6287.
(43) Chekmenev, E. Y.; Hövener, J.; Norton, V. A.; Harris, K.; Batchelder, L. S.; Bhattacharya, P.; Ross, B. D.; Weitekamp, D. P. Pasadena Hyperpolarization of Succinic Acid for MRI and NMR Spectroscopy. *J. Am. Chem. Soc.* **2008**, *130*, 4212−4213.
(44) Bhattacharya, P.; Chekmenev, E. Y.; Reynolds, W. F.; Wagner, S.; Zacharias, N.; Chan, H. R.; Bünger, R.; Ross, B. D. Parahydrogen-Induced Polarization (PHIP) Hyperpolarized MR Receptor Imaging in Vivo: A Pilot Study of ^{13}C Imaging of Atheroma in Mice. *NMR Biomed.* **2011**, *24*, 1023−1028.
(45) Zacharias, N. M.; Chan, H. R.; Sailasuta, N.; Ross, B. D.; Bhattacharya, P. Real-Time Molecular Imaging of Tricarboxylic Acid Cycle Metabolism in Vivo by Hyperpolarized 1-C-13 Diethyl Succinate. *J. Am. Chem. Soc.* **2012**, *134*, 934−943.
(46) Zacharias, N. M.; McCullough, C. R.; Wagner, S.; Sailasuta, N.; Chan, H. R.; Lee, Y.; Hu, J.; Perman, W. H.; Henneberg, C.; Ross, B. D.; et al. Towards Real-Time Metabolic Profiling of Cancer with Hyperpolarized Succinate. *J. Mol. Imaging Dyn.* **2016**, *6*, 123.
(47) Shchepin, R. V.; Coffey, A. M.; Waddell, K. W.; Chekmenev, E. Y. PASADENA Hyperpolarized ^{13}C Phospholactate. *J. Am. Chem. Soc.* **2012**, *134*, 3957−3960.
(48) Shchepin, R. V.; Coffey, A. M.; Waddell, K. W.; Chekmenev, E. Y. Parahydrogen Induced Polarization of 1-^{13}C-Phospholactate-D_2 for Biomedical Imaging with >30,000,000-Fold NMR Signal Enhancement in Water. *Anal. Chem.* **2014**, *86*, 5601−5605.
(49) Shchepin, R. V.; Pham, W.; Chekmenev, E. Y. Dephosphorylation and Biodistribution of 1-^{13}C-Phospholactate in Vivo. *J. Labelled Compd. Radiopharm.* **2014**, *57*, 517−524.
(50) Coffey, A. M.; Shchepin, R. V.; Truong, M. L.; Wilkens, K.; Pham, W.; Chekmenev, E. Y. Open-Source Automated Parahydrogen Hyperpolarizer for Molecular Imaging Using ^{13}C Metabolic Contrast Agents. *Anal. Chem.* **2016**, *88*, 8279−8288.
(51) Borowiak, R.; Schwaderlapp, N.; Huethe, F.; Lickert, T.; Fischer, E.; Bär, S.; Hennig, J.; Elverfeldt, D.; Hövener, J.-B. A Battery-Driven, Low-Field NMR Unit for Thermally and Hyperpolarized Samples. *Magn. Reson. Mater. Phys., Biol. Med.* **2013**, *26*, 491−499.
(52) Schmidt, A. B.; Berner, S.; Schimpf, W.; Müller, C.; Lickert, T.; Schwaderlapp, N.; Knecht, S.; Skinner, J. G.; Dost, A.; Rovedo, P.; et al. Liquid-State Carbon-13 Hyperpolarization Generated in an MRI System for Fast Imaging. *Nat. Commun.* **2017**, *8*, No. 14535.
(53) Reineri, F.; Boi, T.; Aime, S. Parahydrogen Induced Polarization of ^{13}C Carboxylate Resonance in Acetate and Pyruvate. *Nat. Commun.* **2015**, *6*, No. 5858.
(54) Cavallari, E.; Carrera, C.; Aime, S.; Reineri, F. C-13 MR Hyperpolarization of Lactate by Using Parahydrogen and Metabolic Transformation in Vitro. *Chem. − Eur. J.* **2017**, *23*, 1200−1204.

DOI: 10.1021/acsomega.8b00983
ACS Omega 2018, 3, 6673−6682

(55) Cavallari, E.; Carrera, C.; Aime, S.; Reineri, F. Studies to Enhance the Hyperpolarization Level in PHIP-SAH-Produced C13-Pyruvate. *J. Magn. Reson.* **2018**, *289*, 12−17.
(56) Shchepin, R. V.; Barskiy, D. A.; Coffey, A. M.; Esteve, I. V. M.; Chekmenev, E. Y. Efficient Synthesis of Molecular Precursors for Para-Hydrogen-Induced Polarization of Ethyl Acetate-1-^{13}C and Beyond. *Angew. Chem., Int. Ed.* **2016**, *55*, 6071−6074.
(57) Kovtunov, K. V.; Barskiy, D. A.; Salnikov, O. G.; Shchepin, R. V.; Coffey, A. M.; Kovtunova, L. M.; Bukhtiyarov, V. I.; Koptyug, I. V.; Chekmenev, E. Y. Toward Production of Pure ^{13}C Hyperpolarized Metabolites Using Heterogeneous Parahydrogen-Induced Polarization of Ethyl[1-^{13}C]Acetate. *RSC Adv.* **2016**, *6*, 69728−69732.
(58) Kovtunov, K. V.; Barskiy, D. A.; Shchepin, R. V.; Salnikov, O. G.; Prosvirin, I. P.; Bukhtiyarov, A. V.; Kovtunova, L. M.; Bukhtiyarov, V. I.; Koptyug, I. V.; Chekmenev, E. Y. Production of Pure Aqueous ^{13}C-Hyperpolarized Acetate by Heterogeneous Parahydrogen-Induced Polarization. *Chem. − Eur. J.* **2016**, *22*, 16446−16449.
(59) Salnikov, O. G.; Kovtunov, K. V.; Koptyug, I. V. Production of Catalyst-Free Hyperpolarised Ethanol Aqueous Solution Via Heterogeneous Hydrogenation with Parahydrogen. *Sci. Rep.* **2015**, *5*, No. 13930.
(60) Kadlecek, S.; Vahdat, V.; Nakayama, T.; Ng, D.; Emami, K.; Rizi, R. A Simple and Low-Cost Device for Generating Hyperpolarized Contrast Agents Using Parahydrogen. *NMR Biomed.* **2011**, *24*, 933−942.
(61) Coffey, A. M.; Shchepin, R. V.; Feng, B.; Colon, R. D.; Wilkens, K.; Waddell, K. W.; Chekmenev, E. Y. A Pulse Programmable Parahydrogen Polarizer Using a Tunable Electromagnet and Dual Channel NMR Spectrometer. *J. Magn. Reson.* **2017**, *284*, 115−124.
(62) Heaney, F.; Fenlon, J.; O'Mahony, C.; McArdle, P.; Cunningham, D. Alpha-Oximono-Esters as Precursors to Heterocycles - Generation of Oxazinone N-Oxides and Cycloaddition to Alkene Dipolarophiles. *Org. Biomol. Chem.* **2003**, *1*, 4302−4316.
(63) Barskiy, D. A.; Shchepin, R. V.; Coffey, A. M.; Theis, T.; Warren, W. S.; Goodson, B. M.; Chekmenev, E. Y. Over 20% ^{15}N Hyperpolarization in under One Minute for Metronidazole, an Antibiotic and Hypoxia Probe. *J. Am. Chem. Soc.* **2016**, *138*, 8080−8083.
(64) Barskiy, D. A.; Shchepin, R. V.; Tanner, C. P. N.; Colell, J. F. P.; Goodson, B. M.; Theis, T.; Warren, W. S.; Chekmenev, E. Y. The Absence of Quadrupolar Nuclei Facilitates Efficient ^{13}C Hyperpolarization Via Reversible Exchange with Parahydrogen. *ChemPhysChem* **2017**, *18*, 1493−1498.
(65) Shchepin, R. V.; Jaigirdar, L.; Chekmenev, E. Y. Spin-Lattice Relaxation of Hyperpolarized Metronidazole in Signal Amplification by Reversible Exchange in Micro-Tesla Fields. *J. Phys. Chem. C* **2018**, *122*, 4984−4996.
(66) Jeffery, G. H.; Vogel, A. I. Physical Properties and Chemical Constitution. 16. Ethylenic Compounds. *J. Chem. Soc.* **1948**, *133*, 658−673.
(67) Li, G. L.; Zhao, G. Efficient Acetylation of Alcohols and Phenols Catalyzed by Recyclable Lithium Bis(Perfluoroalkylsulfonyl)-Imide. *Synth. Commun.* **2013**, *43*, 34−43.
(68) Louw, R.; Kooyman, E. C. Thermolytic Reactions of Esters. Part III. Pyruvates. *Recl. Trav. Chim. Pays-Bas* **1967**, *86*, 1041−1046.
(69) Rambaud, R.; Vessiere, M. Oxydation, Par Lanhydride Selenieux, De Divers Derives Crotoniques Ou Vinylacetiques. *Bull. Soc. Chim. Fr.* **1961**, 1567.
(70) Bales, L. B.; Kovtunov, K. V.; Barskiy, D. A.; Shchepin, R. V.; Coffey, A. M.; Kovtunova, L. M.; Bukhtiyarov, A. V.; Feldman, M. A.; Bukhtiyarov, V. I.; Chekmenev, E. Y.; et al. Aqueous, Heterogeneous Parahydrogen-Induced ^{15}N Polarization. *J. Phys. Chem. C* **2017**, *121*, 15304−15309.
(71) Gatenby, R. A.; Gillies, R. J. Glycolysis in Cancer: A Potential Target for Therapy. *Int. J. Biochem. Cell Biol.* **2007**, *39*, 1358−1366.
(72) Leupold, J.; Månsson, S.; Petersson, J. S.; Hennig, J.; Wieben, O. Fast Multiecho Balanced SSFP Metabolite Mapping of ^{1}H and Hyperpolarized ^{13}C Compounds. *Magn. Reson. Mater. Phys., Biol. Med.* **2009**, *22*, 251−256.
(73) Harrison, C.; Merritt, M.; Storey, C.; Jeffrey, M.; Sherry, A.; Malloy, C. Production of Hyperpolarized C-13-Bicarbonate from C-13-Pyruvate Measures Flux through Pyruvate Dehydrogenase but Not the Tricarboxylic Acid Cycle. *Circulation* **2007**, *116*, 120.
(74) Golman, K.; Petersson, J. S. Metabolic Imaging and Other Applications of Hyperpolarized C-13. *Acad. Radiol.* **2006**, *13*, 932−942.
(75) Liu, Q. S.; Takemura, F.; Yabe, A. Solubility of Hydrogen in Liquid Methanol and Methyl Formate at 28 °C to 140 °C. *J. Chem. Eng. Data* **1996**, *41*, 1141−1143.
(76) Purwanto; Deshpande, R. M.; Chaudhari, R. V.; Delmas, H. Solubility of Hydrogen, Carbon Monoxide, and 1-Octene in Various Solvents and Solvent Mixtures. *J. Chem. Eng. Data* **1996**, *41*, 1414−1417.
(77) Herskowitz, M.; Wisniak, J.; Skladman, L. Hydrogen Solubility in Organic Liquids. *J. Chem. Eng. Data* **1983**, *28*, 164−166.
(78) Radhakrishnan, K.; Ramachandran, P. A.; Brahme, P. H.; Chaudhari, R. V. Solubility of Hydrogen in Methanol, Nitrobenzene, and Their Mixtures - Experimental Data and Correlation. *J. Chem. Eng. Data* **1983**, *28*, 1−4.
(79) Brunner, E. Solubility of Hydrogen in 10 Organic Solvents at 298.15-K, 323.15-K, and 373.15-K. *J. Chem. Eng. Data* **1985**, *30*, 269−273.
(80) Barskiy, D. A.; Salnikov, O. G.; Shchepin, R. V.; Feldman, M. A.; Coffey, A. M.; Kovtunov, K. V.; Koptyug, I. V.; Chekmenev, E. Y. NMR SLIC Sensing of Hydrogenation Reactions Using Parahydrogen in Low Magnetic Fields. *J. Phys. Chem. C* **2016**, *120*, 29098−29106.
(81) Truong, M. L.; Shi, F.; He, P.; Yuan, B.; Plunkett, K. N.; Coffey, A. M.; Shchepin, R. V.; Barskiy, D. A.; Kovtunov, K. V.; Koptyug, I. V.; et al. Irreversible Catalyst Activation Enables Hyperpolarization and Water Solubility for NMR Signal Amplification by Reversible Exchange. *J. Phys. Chem. B* **2014**, *118*, 13882−13889.
(82) Waddell, K. W.; Coffey, A. M.; Chekmenev, E. Y. In Situ Detection of Phip at 48 mT: Demonstration Using a Centrally Controlled Polarizer. *J. Am. Chem. Soc.* **2011**, *133*, 97−101.
(83) Coffey, A. M.; Shchepin, R. V.; Wilkens, K.; Waddell, K. W.; Chekmenev, E. Y. A Large Volume Double Channel ^{1}H-X RF Probe for Hyperpolarized Magnetic Resonance at 0.0475 Tesla. *J. Magn. Reson.* **2012**, *220*, 94−101.
(84) Hövener, J.-B.; Chekmenev, E. Y.; Harris, K. C.; Perman, W.; Robertson, L.; Ross, B. D.; Bhattacharya, P. PASADENA Hyperpolarization of ^{13}C Biomolecules: Equipment Design and Installation. *Magn. Reson. Mater. Phys., Biol. Med.* **2009**, *22*, 111−121.
(85) Yoshihara, H. A. I.; Can, E.; Karlsson, M.; Lerche, M. H.; Schwitter, J.; Comment, A. High-Field Dissolution Dynamic Nuclear Polarization of [1-^{13}C]Pyruvic Acid. *Phys. Chem. Chem. Phys.* **2016**, *18*, 12409−12413.
(86) Cheng, T.; Capozzi, A.; Takado, Y.; Balzan, R.; Comment, A. Over 35% Liquid-State ^{13}C Polarization Obtained Via Dissolution Dynamic Nuclear Polarization at 7 T and 1 K Using Ubiquitous Nitroxyl Radicals. *Phys. Chem. Chem. Phys.* **2013**, *15*, 20819−20822.

DOI: 10.1021/acsomega.8b00983
ACS Omega 2018, 3, 6673−6682